

Submitted to the
XXII International Symposium on Lepton-Photon Interactions
at High Energy
June 30 - July 5, 2005, Uppsala, Sweden

Abstract: 283

Session: QCD/HS

Charged multiplicity distributions in deep inelastic scattering at HERA

ZEUS Collaboration

Abstract

The hadronic final state has been investigated in inclusive neutral current deep inelastic ep scattering with the ZEUS detector at HERA, using an integrated luminosity of 38.6 pb^{-1} . The mean charged multiplicity has been measured for the hadrons belonging to the current region of the Breit frame, as well as for those belonging to the photon (current) fragmentation region of the hadronic centre-of-mass frame (HCM). The results are compared to leading-logarithm parton-shower Monte Carlo predictions as well as to results of e^+e^- and pp measurements.

1 Introduction

The measurements of multiplicities of charged particles at colliders have yielded insights into hadronisation mechanisms. It has been found that charged particle multiplicities measured as a function of the centre-of-mass (cms) energy, \sqrt{s} , at e^+e^- [1] colliders are the same as those measured at pp [2] colliders as a function of $\sqrt{q_{\text{tot}}^{\text{had}}} = \sqrt{[(q_1^{\text{inc}} - q_1^{\text{leading}}) + (q_2^{\text{inc}} - q_2^{\text{leading}})]^2}$, where $q_{1,2}^{\text{inc}}$ and $q_{1,2}^{\text{leading}}$ are the four-momenta of the incoming protons and leading particles that escape down the beam pipe, respectively. It is therefore interesting to study charged particle multiplicities in ep collisions.

At the HERA ep collider, because of the large asymmetry between the e -beam and p -beam energies, a large part of the final hadronic system produced near the proton falls outside the region of acceptance of the detectors. Therefore, to perform studies similar to e^+e^- and pp also in ep collisions at HERA, only hadrons belonging to the photon (current) fragmentation region of the hadronic centre-of-mass (HCM) frame and to the current region of the Breit frame were used.

2 Experimental set-up

The data were collected with the ZEUS detector during the 1996 and 1997 running periods, when HERA operated with protons of energy $E_p = 820$ GeV and positrons of energy $E_e = 27.5$ GeV, and correspond to an integrated luminosity of 38.6 ± 0.6 pb $^{-1}$.

The ZEUS detector is described in detail elsewhere [3]. The most important components used in the current analysis are the central tracking detector and the uranium-scintillator calorimeter.

Charged particles are tracked in the central tracking detector (CTD) [4], which operates in a magnetic field of 1.43 T provided by a thin superconducting coil. The CTD consists of 72 cylindrical drift chamber layers, organised in 9 superlayers covering the polar-angle¹ region $15^\circ < \theta < 164^\circ$. The transverse-momentum resolution for full-length tracks is $\sigma(p_T)/p_T = 0.0058p_T \oplus 0.0065 \oplus 0.0014/p_T$, with p_T in GeV.

The high-resolution uranium-scintillator calorimeter (CAL) [5] consists of three parts: the forward (FCAL), the barrel (BCAL) and the rear (RCAL) calorimeters. Each part is subdivided transversely into towers and longitudinally into one electromagnetic section (EMC) and either one (in RCAL) or two (in BCAL and FCAL) hadronic sections

¹ The ZEUS coordinate system is a right-handed Cartesian system, with the Z axis pointing in the proton beam direction, referred to as the “forward direction”, and the X axis pointing left towards the centre of HERA. The coordinate origin is at the nominal interaction point.

(HAC). The smallest subdivision of the calorimeter is called a cell. The CAL energy resolutions, as measured under test-beam conditions, are $\sigma(E)/E = 0.18/\sqrt{E}$ for electrons and $\sigma(E)/E = 0.35/\sqrt{E}$ for hadrons (E in GeV).

3 Data selection

Deep inelastic scattering (DIS) events were selected by requiring that the outgoing positron was measured in the CAL. The scattered-positron identification is based on a neural-network algorithm using the CAL information [6].

For the reconstruction of the photon virtuality, Q^2 , Bjorken x , and the γ^*P centre-of-mass energy, W , the double angle method (DA) was chosen, in which the scattered-positron angle, θ_e , and the angle γ_H are used [7]. In the naive quark-parton model, γ_H is the angle of the scattered massless quark in the laboratory frame. Variables calculated by electron method (e) [7, 8] from the measurements of the energy, $E_{e'}$, and angle, $\theta_{e'}$, of the scattered positron and by the Jacquet-Blondel (JB) method [9] from the hadronic system measurements were used only in the event selection.

The event selection criteria were:

- $E_{e'} > 12$ GeV, where ($E_{e'}$ is the corrected energy of the scattered positron), to select neutral current DIS events;
- $y_e \leq 0.95$, where y_e is the scaling variable y as determined from the energy and polar angle of the scattered positron, to reduce the photoproduction background;
- $y_{\text{JB}} \geq 0.04$, where $y_{\text{JB}} = \sum_h (E_h - P_{Z_h})/2E_e$ and the sum runs over all the observed hadrons, E_h and P_{Z_h} are the energies and longitudinal momenta of these hadrons correspondingly, to guarantee sufficient accuracy for the DA reconstruction method;
- $35 \leq \delta \leq 60$ GeV, where $\delta = \sum_i (E_i - P_{Z_i})$ and the sum runs over the energies and longitudinal momenta of all calorimeter cells. This cut removes photoproduction events and events with large radiative corrections;
- events were accepted only if the impact position of the scattered positron on the CAL satisfied $\sqrt{X^2 + Y^2} > 25$ cm to ensure that the positron is fully contained within the detector and its position reconstructed with sufficient accuracy;
- $|Z_{\text{vertex}}| < 50$ cm to reduce background events from non ep -collisions;
- events with $\eta^{\text{max}} > 3.2$ were rejected to reduce diffractive contributions, where η^{max} is the pseudorapidity of the most forward energy deposit in the CAL.

The track selection was as follows:

- the reconstructed tracks were associated with the primary event vertex;
- the tracks were required to have $p_T > 150$ MeV to reduce errors due to misreconstruction;
- $|\eta_{\text{lab}}| < 1.75$, where η is the pseudorapidity of the measured track. This cut restricts the analysis to a region of high CTD acceptance where the detector response and systematics are best understood.

The analysis is restricted to the range $Q^2 > 25$ GeV² and $70 < W < 225$ GeV.

For this analysis, the CTD was used to measure the charged-particle multiplicity and the CAL to measure the energy of the final-state hadrons, charged and neutral. The calorimeter cells and the track assigned to the scattered positron were not used in these measurements.

In the Breit frame, the exchanged virtual boson is purely spacelike, with three-momentum $\mathbf{q} = (0,0,-Q)$. The particles produced in the interaction can be assigned to one of two regions: the current region if their longitudinal momentum in the Breit frame is negative, and the target region if their longitudinal momentum is positive. The hadronic system of the current region used in this analysis is almost fully (about 95%) contained within the acceptance of the CTD.

For the HCM frame the final particles are separated into the photon (current) and proton (target) fragmentation regions. The target region of the HCM can not be observed in the CTD and only 60-80% of the hadrons belonging to the photon (current) region are detected.

The boost to the corresponding frames was performed using the positron four-momentum as reconstructed using the DA method.

4 Monte Carlo models, acceptance corrections and systematic errors

Samples of neutral current DIS events were generated using the HERACLES 4.6.1 [10] MC program with the DJANGO 1.1 [11] interface to the hadronisation programs. The QCD cascade is simulated using the colour-dipole model as implemented in ARIADNE 4.08 [12] or with the MEPS model of LEPTO 6.5 [13]. Both ARIADNE and LEPTO use the Lund string model [14] for the hadronisation. All event samples were generated using the CTEQ4D parameterisation of the parton distribution functions in the proton. The generated hadron distributions do not include charged particles produced from weak decays

with lifetimes below $3 \cdot 10^{-10}$ seconds. The charged-particle decay products of K_S^0 and Λ were excluded.

The MC event samples were passed through reconstruction and selection procedures identical to those for the data. Monte Carlo studies were used to determine the event and track acceptances in the selected kinematic region of Q^2 and W^2 .

The corrections applied to the data accounted for the effects of acceptance and resolution of the detector, event selection cuts, QED-radiative effects, track reconstruction, track selection cuts, the decay products of K_S^0 and Λ which were assigned to the primary vertex, and energy losses in the inactive material in front of the calorimeter in the case of the energy measurement.

Two different correction procedures for the multiplicity distributions were used. One of them is based on the matrix unfolding method as used in earlier studies [15]. The second is a bin-by-bin method. Both methods give similar results. The difference between them is included as a systematic uncertainty.

The dominant sources of systematic uncertainties were investigated. The main uncertainty for the W measurement arises from different MC models used in the correction procedure and it amounts to up to 5%. To reduce the uncertainty the average correction factor between ARIADNE and LEPTO was taken, thus reducing the uncertainty by a factor of 2. For the Breit frame measurement this uncertainty is typically below 0.5%. Other sources of uncertainties are (typical values of the uncertainties are shown in brackets): uncertainty in the CAL energy scale (0.5 – 1.1%), event reconstruction and selection (< 0.5%), track reconstruction and selection (< 0.5%) and method of correction (matrix or modified bin-by-bin, 0.6 – 1.3%). The contaminations due to migrations from $Q^2 < 25\text{GeV}^2$ and from diffractive events are negligible.

5 Results

The current region of the Breit frame is analogous to a single hemisphere of e^+e^- annihilation. In $e^+e^- \rightarrow q\bar{q}$ the two quarks are produced with equal and opposite momenta, $\pm\sqrt{s_{ee}}/2$. The fragmentation of these quarks can be compared to that of the quark struck from the proton in DIS. This quark has an outgoing momentum $-Q/2$ in the Breit frame. The multiplicity of the current region of the Breit frame is expected to have a dependence on Q similar to that in e^+e^- annihilation versus the energy $\sqrt{s_{ee}} = Q$. To take into account contributions from soft and hard QCD processes that lead to a decrease of the energy and the number of particles in the current region of the Breit frame, in this analysis $2E_{\text{current}}$ was used instead of Q , where E_{current} is the energy of all the particles in the current region of the Breit frame.

For the photon (current) fragmentation region of the HCM frame the total number of charged particles can be studied as a function of W . Additional study of the energy in this region demonstrated that there is no significant migrations from the photon (current) to the target region and the variable W can be safely used.

Figure 1 shows the measured mean charged multiplicity, $\langle n_{\text{ch}} \rangle$, in the photon (current) region of the HCM frame as a function of W . The measurements as a function of W can be only performed at high W , because of the acceptance of the ZEUS detector. The prediction of ARIADNE and LEPTO are also shown.

To compare the results of measurements in the Breit and HCM frame with results of the e^+e^- and pp experiments the mean charge multiplicity was multiplied by 2. Figure 2 shows twice the measured mean charged multiplicity, $2\langle n_{\text{ch}} \rangle$, in the current region of the Breit frame plotted versus $2E_{\text{current}}$ and twice the measured mean charged multiplicity in the photon (current) region of the HCM frame plotted versus W . Also shown are the predictions of ARIADNE, LEPTO and the measurements from e^+e^- [1, 16] and pp [2] experiments together with a previous ZEUS measurement in the current region of the Breit frame [17]. For the previous ZEUS measurement, $2 \cdot \langle n_{\text{ch}} \rangle$ is measured as a function of Q .

The ZEUS measurements presented in this paper agree with the e^+e^- and pp measurements. At low values of energy, the measurement as a function of $2E_{\text{current}}$ agrees better with e^+e^- than the measurement as a function of Q , since the migrations of final state particles out of the current region are larger at the low values of energy and they are properly taken into account in E_{current} .

References

- [1] MARK I Coll., V. Luth et al., Phys. Lett. **B 70**, 120 (1977);
JADE Coll., W. Bartel et al., Z. Phys. **C 20**, 187 (1983);
PLUTO Coll., Ch. Berger et al., Phys. Lett. **B 95**, 313 (1980);
TASSO Coll., W. Braunschweig et al., Z. Phys. **C 45**, 193 (1989).
- [2] M. Basile et al., Nuovo Cimento **A 67**, 244 (1982);
M. Basile et al., Lettere al Nuovo Cimento 41 **N. 9**, 293 (1984).
- [3] ZEUS Coll., U. Holm (ed.), *The ZEUS Detector*. Status Report (unpublished),
DESY (1993), available on <http://www-zeus.desy.de/bluebook/bluebook.html>.
- [4] N. Harnew et al., Nucl. Inst. Meth. **A 279**, 290 (1989);
B. Foster et al., Nucl. Phys. Proc. Suppl. **B 32**, 181 (1993);
B. Foster et al., Nucl. Inst. Meth. **A 338**, 254 (1994).
- [5] M. Derrick et al., Nucl. Inst. Meth. **A 309**, 77 (1991);
A. Andresen et al., Nucl. Inst. Meth. **A 309**, 101 (1991);
A. Caldwell et al., Nucl. Inst. Meth. **A 321**, 356 (1992);
A. Bernstein et al., Nucl. Inst. Meth. **A 336**, 23 (1993).
- [6] H. Abramowicz, A. Caldwell and R. Sinkus, Nucl. Inst. Meth. **A 365**, 508 (1995).
- [7] S. Bentvelsen, J. Engelen and P. Kooijman, *Proc. Workshop on Physics at HERA*,
W. Buchmüller and G. Ingelman (eds.), Vol. 1, p. 23. Hamburg, Germany, DESY
(1992).
- [8] K.C. Höger, *Proc. Workshop on Physics at HERA*, W. Buchmüller and
G. Ingelman (eds.), Vol. 1, p. 43. Hamburg, Germany, DESY (1992).
- [9] F. Jacquet and A. Blondel, *Proc. the Study of an eP Facility for Europe*,
U. Amaldi (ed.), p. 391. (1979). Also in preprint DESY 79-48.
- [10] A. Kwiatkowski, H. Spiesberger and H.-J. Möhring, Comp. Phys. Comm.
69, 155 (1992). Also in *Proc. Workshop Physics at HERA*, 1991, DESY, Hamburg;
H. Spiesberger, *An Event Generator for ep Interactions at HERA Including
Radiative Processes (Version 4.6)*, 1996, available on
<http://www.desy.de/~hspiesb/heracles.html>.
- [11] H. Spiesberger, *HERACLES and DJANGO: Event Generation for ep Interactions at
HERA Including Radiative Processes*, 1998, available on
<http://www.desy.de/~hspiesb/djangoh.html>;
K. Charchula, G.A. Schuler and H. Spiesberger, Comp. Phys. Comm.
81, 381 (1994).
- [12] L. Lönnblad, Comp. Phys. Comm. **71**, 15 (1992).

- [13] G. Ingelman, A. Edin and J. Rathsman, *Comp. Phys. Comm.* **101**, 108 (1997).
- [14] B. Andersson et al., *Phys. Rep.* **97**, 31 (1983).
- [15] ZEUS Coll., M. Derrick et al., *Z. Phys.* **C 67**, 93 (1995).
- [16] Aleph Coll., D. Decamp et al., *Phys. Lett.* **B 273**, 181 (1991);
Aleph Coll., D. Buskulic et al., *Z. Phys.* **C 73**, 409 (1997);
Delphi Coll., P. Abreu et al., *Z. Phys.* **C 50** (1991);
Delphi Coll., P. Abreu et al., *Phys. Lett.* **B 372**, 172 (1996);
Delphi Coll., P. Abreu et al., *Phys. Lett.* **B 416**, 233 (1998);
Delphi Coll., P. Abreu et al., *Eur. Phys. J.* **C 18**, 203 (2000);
L3 Coll., P. Achard et al., *Phys. Lett.* **B 577**, 109 (2003);
L3 Coll., M. Acciarri et al., *Phys. Lett.* **B 371**, 137 (1996);
L3 Coll., M. Acciarri et al., *Phys. Lett.* **B 404**, 390 (1997);
L3 Coll., M. Acciarri et al., *Phys. Lett.* **B 444**, 569 (1998);
Opal Coll., P. D. Acton et al., *Z. Phys.* **C 35**, 539 (1991);
Opal Coll., G. Alexander et al., *Z. Phys.* **C 72**, 191 (1996);
Opal Coll., K. Ackerstaff, *Z. Phys.* **C 75**, 193 (1997);
Opal Coll., G. Abbiendi et al., *Eur. Phys. J.* **C 16**, 185 (1999).
- [17] ZEUS Coll., J. Breitweg et al., *Eur. Phys. J.* **C 11**, 251 (1999).

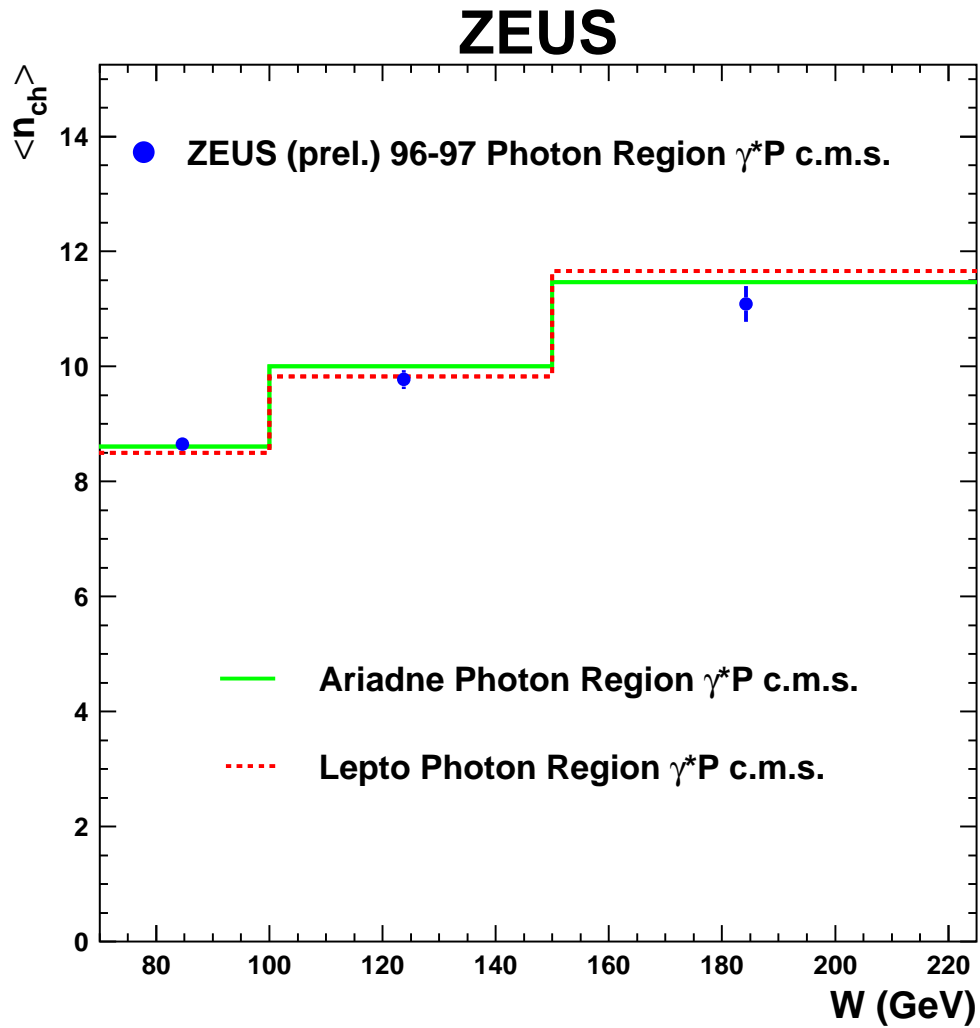


Figure 1: Mean charged multiplicity, $\langle n_{\text{ch}} \rangle$, in the photon (current) fragmentation region of the HCM as a function of W . Also shown are the predictions from ARIADNE and LEPTO.

ZEUS

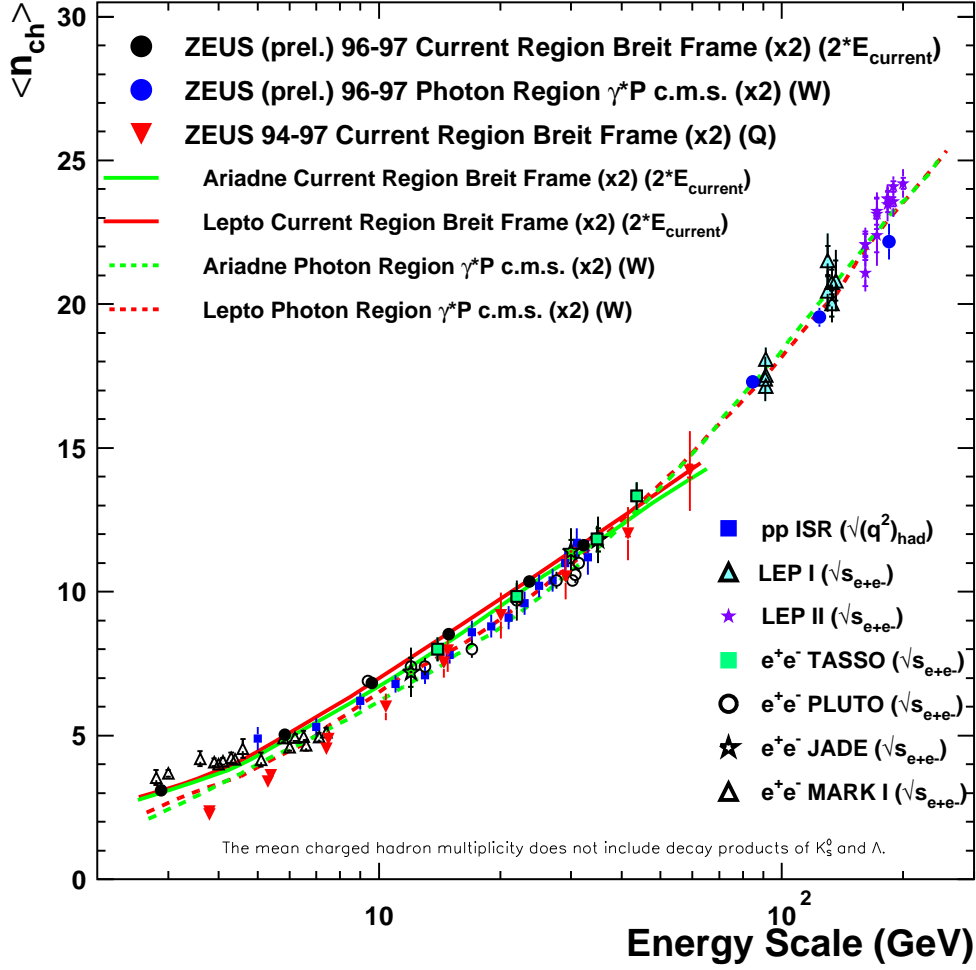


Figure 2: Mean charged multiplicity, $\langle n_{ch} \rangle$, in the current region of the Breit frame multiplied by 2 plotted versus $2E_{\text{current}}$, where E_{current} is the sum of the energies of the particles (charged and neutral) in the current region. The blue dots represent the $\langle n_{ch} \rangle$ in the photon (current) region of the HCM frame, multiplied by 2, plotted versus W . The downward triangles show the ZEUS measurement of ref. [17]. The prediction of the ARIADNE and the LEPTO, as well as the measurements of pp and e^+e^- interactions are also shown.